

**PRODUCTION AND UTILIZATION OF  
POROUS HOLLOW EPOXY BY WATER-BASED METHOD  
AS AN ADVANCED FILLER**

**by**

**DU NGOC UY LAN**

**Thesis submitted in fulfillment of the requirements  
for the degree of  
Doctor of Philosophy**

**December 2009**

## **DEDICATION**

**Con kính dâng Ông Bà, Ba Má  
cùng các Anh Chị Em  
và các cháu**

## ACKNOWLEDGEMENTS

I wish to express my profound gratitude to Assoc. Prof. Dr. Azhar Abu Bakar for his supervision throughout the period of this study. I also wish to express my sincere gratitude to Assoc. Prof. Dr. Baharin Azahari, my co-supervisor who always advices bright instruction for my research. During this study, I am under an obligation to Dr. Zulkifli Mohamad Ariff who is more than a supervisor but a truly friend to me and help me overcome hard situations. I spent one year study in Kyoto University, Japan and I am in debt of gratitude to Prof. Yoshiki Chujo for his supervision and advices. Honestly, during the time in Kyoto, without the helps from Dr. Shingo Hadano, the work of suspension polymerization could not be well done. All of their valuable advices, constant guidance, willingness and encouragement are inestimable. It has been truly memorable and educative being a researcher under their supervision.

I owe sincere thanks to Prof. Radzali b. Othman, who encouraged me to take this scholarship for my PhD. I would like to thank to Prof. Dr. Khairun Azizi Binti Mohd Azizli, Assoc. Prof. Dr. Azizan b. Aziz, Prof. Ahmad Fauzi b. Mohd Noor and all the management staff in the School of Material and Mineral Resources Engineering and all the lecturers in Polymer Engineering Section. I express appreciation to En. Mohd. Faizal b. Mohd. Kassim, En. Abd. Rashid bin Selamat, En. Mohammad b. Hassan, En. Rokman b. Mat Nasir, En. Shahril Amir b. Saleh, En. Muhamad Fitri b. Ab Hadi, En. Mokhtar Mohamad, Madam Fong Lee Lee, Puan Haslina bt. Zulkifli, Ms. Mahani bt. Mohd. and Ms. Hasnah bt. Awang for their assistance and co-operation in lab works.

I owe sincere appreciation to Mr. Gnanasegaran a/l N. B. Dorai and his family for their kindness and care. It has been happy being a member in his family. I

acknowledged Dr. Pham Thi Hao and Assoc. Prof. Dr. Mariati Jaafar @ Mustapha for their advice, knowledge sharing and kindness.

Friendship developed with the entire friend in Polymer group and USM, I would like to express my sincere thank to Cao Xuan Viet, Pham Trung Kien, Zunaida Zakaria, Nor Nadirah Najib, Sri Raj Rajeswari, Ong Hui Lin, and all my AUN/Seed Net friends for their moral support and advice. All of them must be appreciated for helping me to survive and enjoy in a foreign country. I wish them all to achieve their goals successfully.

I am particularly grateful to AUN/SEED–Net/JICA for the financial support through Collaborative Research (CR) grant and opportunity for this postgraduate study. I specially thank to Mr. Yamada, Ms. Miyashita – JICA in Osaka – Japan for their kindness and continuous guidance and support.

Respectfully, I would like to send my deepest gratefulness to my grandmother, my parents, my brothers and sisters, my nieces and nephews and my relatives for their patient support, motivation, and encouragement. To me, my family is my faith and my spirit.

## **TABLE OF CONTENTS**

ACKNOWLEDGEMENTS	iii
TABLE OF CONTENTS	v
LIST OF TABLES	xv
LIST OF FIGURES	xvii
LIST OF ABBREVIATION	xxiv
ABSTRAK	xxviii
ABSTRACT	xxx

## **CHAPTER I. INTRODUCTION**

1.1	Overview	1
1.2	Multiporous hollow particles	2
1.3	Problem statement	3
1.3.1	Common porous hollow particles	3
1.3.2	Chemically induced phase separation	4
1.4	Porous hollow epoxy	4
1.3	Objectives of the study	6

## **CHAPTER II. BACKGROUND AND LITERATURE REVIEW**

2.1	Fillers	7
2.1.1	Functions of filler in composites	7
2.1.2	Type of fillers	7
2.1.3	Filler properties	8

2.1.4	Interaction	12
2.1.5	Porous hollow particles	16
2.2	Epoxy and Polyamide	23
2.2.1	Epoxy	23
2.2.2	Curing with polyamide	24
2.3	Composites	28
2.3.1	Composite processing	28
2.3.1.1	Processing of Elastomer composites	28
2.3.1.2	Processing of thermoplastic composites	31
2.3.2	In-situ polymerization	33
2.3.2.1	Suspension polymerization	33
2.3.2.2	Sol-gel methods	35
2.4	Toughness and toughening mechanism	38
2.4.1	Fracture	38
2.4.2	Rubber and thermoplastic toughened epoxy	40
2.4.3	Epoxy particles toughened thernoplastic	43
2.5	Phase separation	44
2.6	Emulsion and Coalescence	46
2.6.1	Emulsion	46
2.6.2	Coalescence	48
2.7	Summary	50

## **CHAPTER III. EXPERIMENTAL**

3.1	Production of epoxy particles by water-based method	52
-----	---	----

3.1.1	Materials	52
3.1.1.1	Epoxy	52
3.1.1.2	Polyamide	52
3.1.1.3	Calcium carbonate and Hydrochloric acid	53
3.1.2	Water-based method	53
3.1.2.1	Epoxy compounds	53
3.1.2.2	Equipments	54
3.1.2.3	Process of producing porous hollow epoxy	54
3.1.2.4	Effect of homogenizing factors (temperature, speed and time) and curing temperature on the formation of porous hollow structure	54
3.1.2.5	Effect of CaCO <sub>3</sub> content	54
3.2	Utilization of PHE filler in composite	57
3.2.1	Elastomers – PHE composites	57
3.2.1.1	Elastomer materials	59
i.	Natural rubber latex compound	59
ii.	Natural rubber and Epoxidised natural rubber – ENR 50	59
3.2.1.2	Elastomer blending	60
i.	NR latex casting	60
ii.	Rubber blending by two-roll mill	60
3.2.2	Thermoset – PHE composites	62
3.2.2.1	Polyamine hardener	62
3.2.2.2	Epoxy-polyamine casting	62
3.2.3.	Thermoplastic – PHE composites	62
3.2.3.1	Thermoplastic materials	62
i.	Linear low density polyethylene – LLDPE	62

ii.	Polystyrene – PS	63
iii.	Poly(methyl methacrylate) – PMMA	63
3.2.3.2	Blending methodology	63
i.	Brabender internal mixer	63
ii.	Haake internal mixer	64
3.3.	In-situ Polymerization	65
3.3.1	In-situ suspension polymerization	65
3.3.1.1	Monomer for polymerization	65
i.	Styrene monomer	65
ii.	Methyl methacrylate	65
iii.	Dispersing agent and catalysts	66
3.3.1.2	Suspension methodology	66
3.3.2	Sol-gel methods	69
3.3.2.1	Alkoxysilane monomers	69
3.3.2.2	Sol-gel methods	69
i.	Compound	69
ii.	Sol-gel process	69
3.4	Effect of size and interlocking holes of PHE on composites	70
3.4.1	Sieving and classifying PHE sizes	70
3.4.2	Polymerization of two sizes of PHE and MMA	70
3.4.3	Blending of PMMA and PHE in different sizes	70
3.5	Characterization	71
3.5.1	Dynamic viscosity	71
3.5.2	Physical properties of PHECa and PHE	72
	Density, Particle sizes and Surface area – BET	72



3.5.3	Rubber curing characteristics	72
3.5.4	Rubber hardness	73
3.5.5	Mechanical test	73
	i.    Tensile test	73
	ii.   Tear test ASTM D624	74
3.5.6	Scanning Electron Microscope – SEM	74
3.5.7	Thermal analysis	75
	i.    Differential scanning calorimetry – DSC	75
	ii.   Thermogravimetric analysis – TGA	75
3.5.8	X-ray diffraction – XRD	75
3.5.9	Physical properties of in-situ polymerized composite	76
	i.    Sohxlet extraction	76
	ii.   Gel Permeation Chromatography – GPC	76
	iii.  Fourier transfer infrared spectroscopy – FTIR	76

## **CHAPTER IV. RESULTS AND DISCUSSION**

4.1	Porous hollow epoxy by water-based method	77
4.1.1	Production of porous hollow epoxy	77
4.1.1.1	Effect of homogenizing temperature	77
4.1.1.2	Effect of homogenizing speed to epoxy particles	81
4.1.1.3	Effect of homogenizing time to epoxy particles	82
4.1.1.4	Effect of curing temperature	84
4.1.1.5	Effect of calcium carbonate content	84
4.1.1.6	Producing PHE of high content polyamide hardener compound at different CaCO <sub>3</sub> loading	85

4.1.1.7	Mechanism of formation of porous hollow structure	87
i.	Role of homogenizing process	87
ii.	Role of calcium carbonate	88
iii.	Effect of curing rate to equilibrium of epoxy emulsion	90
iv.	Prerequisite conditions	93
4.1.2	Characterization	95
4.1.2.1	Density	95
4.1.2.2	Particles sizes	96
4.1.2.3	Surface area – BET	97
4.1.2.4	Thermal properties	99
i.	DSC of PHE	99
ii.	TGA of PHE	100
4.2	Utilization of PHE as filler in composites	101
4.2.1	Elastomer – PHE composites	101
4.2.1.1	Natural rubber latex	101
i.	Interlocking of PHE and NR latex	101
ii.	Tensile properties of PHE-NR latex	101
iii.	Tensile fracture surface	104
4.2.1.2	Natural rubber and Epoxidised natural rubber	105
i.	Curing characteristic	105
ii.	Hardness	108
iii.	Tensile strength	108
iv.	Tensile fracture surface	112
v.	Tear strength	112

vi.	Tear fracture surface	115
4.2.2	Thermoset – PHE composites	116
4.2.2.1	Interlocking	116
4.2.2.2	Tensile properties	116
4.2.2.3	Tensile fracture surface	118
4.2.3	Thermoplastic – PHE composites	119
4.2.3.1	PHE-LLDPE composites	119
i.	Interlocking	119
ii.	Tensile properties	120
iii.	Tensile fracture surface	122
iv.	DSC properties of PHE-LLDPE composites	123
4.2.3.2	PHE-PS composites	124
i.	Torque of PS – epoxy blend	124
ii.	Tensile properties	126
iii.	Tensile fracture surface	128
iv.	DSC of PHE-PS composites	129
v.	TGA of PHE-PS composites	129
4.2.3.3	PHE-PMMA composites	131
i.	Torque of PMMA – epoxy blend	133
ii.	Tensile properties	133
iii.	Tensile fracture surfaces	135
iv.	DSC of PHE-PMMA composites	136
4.2.3.4	Summary of mechanical of PHE filled polymer matrixes	137
4.3	In-situ Polymerization	139
4.3.1	In-situ suspension polymerization	139

4.3.1.1	pPS-PHE and Ppmma-PHE composite beads	139
i.	Effect of AIBN and BPO on in-situ suspension polymerization with the presence of PHE	140
ii.	Interlocking of pPS-PHE beads and pPMMA-PHE beads	144
4.3.1.2	Sohlex extraction and Solvent resistance properties	144
4.3.1.4	Molecular weight of pPS-PHE and pPMMA-PHE beads	145
4.3.1.5	FTIR	149
4.3.1.6	DSC	151
i.	DSC of pPS-PHE composites	151
ii.	DSC of pPMMA-PHE composites	153
4.3.1.7	TGA	155
i.	TGA of pPS-PHE composites	155
ii.	TGA of pPMMA-PHE composites	157
4.3.1.8	XRD	159
4.3.2	Sol-gel	160
4.3.2.1	Interlocking	160
4.3.2.2	DSC of silica-PHE	164
4.3.2.3	TGA of silica-PHE	166
4.3.2.4	SEM micrograph of silica interlocked PHE before and after TGA	172
4.4	Effect of particle size of PHE	175
4.4.1	Morphology of PHE in different sizes	175
4.4.2	Surface area of PHE38, PHE53 and PHE75	175
4.4.3	In-situ suspension polymerization of PHE and MMA	174
4.4.3.1	Sohlex extraction and Molecular weight	179

i.	Sohlex extraction	179
ii.	Molecular weight of 38MEB and 75MEB	180
4.4.3.2	FTIR	182
4.4.3.3	DSC of 38MEB and 75MEB	183
4.4.3.4	TGA of 38MEB and 75MEB	184
4.4.4	Blending of PMMA and PHE	186
4.4.4.1	Torque curves	186
4.4.4.2	Tensile properties	186
4.4.4.3	Tensile fracture surface	188
4.4.4.4	DSC properties of 38ME, 53ME and 75ME	190
4.5	Proposal of interlocking mechanism and fibrillation and ductile deformation in composites under tensile loading	192
4.5.1	Fibrillation of LLDPE composite	192
4.5.2	Suggestion interlocking mechanism under tensile loading	193
4.5.3	Deformation mode under tensile loading	194
4.5.3.1	Pulling out of the interlocking matrix	194
4.5.3.2	Breaking at the neck of the interlocking matrix	195
4.5.3.3	Breaking the PHE particle	196

## **CHAPTER V. CONCLUSION AND SUGGESTION**

5.1	Production of porous hollow epoxy particle	197
5.2	Composite processing, in-situ polymerization and sol-gel process	198
5.3	Interlocking and failure mode of interlocking in composite	199
5.3.1	Interlocking	199
5.3.2	Failure mode of interlocking	199
5.4	Effect of particle size and hole's morphology of porous hollow epoxy	200

5.5	Suggestion	201
-----	------------	-----

<b>REFERENCES</b>	202
-------------------	-----

## **APPENDICES**

APPENDIX A	Supplements for Chapter III and Chapter IV
APPENDIX B	List of International Journal
APPENDIX C	List of International and National Conference

## LIST OF TABLES

Table 3.1	Properties of epoxy resin 331	52
Table 3.2	Properties of epoxy hardener A062	52
Table 3.3	Investigated factors of homogenization and curing process	56
Table 3.4	Epoxy compound with variation in $\text{CaCO}_3$ content	57
Table 3.5	Additives and vulcanization system of PHE-NR/ENR composites.	59
Table 3.6	Formula and nomination of NR latex compounds	60
Table 3.7	NR/ ENR-PHE composites recipes	61
Table 3.8	Compound in weight % of epoxy – PHE composites	62
Table 3.9	Compound of PHE-LLDPE composites	63
Table 3.10	Compound of PS/PMMA-PHE composites	64
Table 3.11	In-situ Suspension Polymerization of Styrene and Methyl Methacrylate with PHE	68
Table 3.12	Alkoxysilane information of sol-gel process	69
Table 3.13	Compound of silica-PHE hybrid by sol-gel methods	70
Table 3.14	PHE of different sizes in in-situ polymerization and melting blending	71
Table 3.15	Tensile testing condition of PHE composites	74
Table 4.1	Estimated energy required to heat the emulsion to $80^\circ\text{C}$ . (KJ)	80
Table 4.2	Effect of $\text{CaCO}_3$ and curing temperature on hole formation of epoxy particles.	94
Table 4.3	Partical size of PHE (after HCl treatment) at different $\text{CaCO}_3$ loading	96
Table 4.4	Surface area properties of PHE	98
Table 4.5	Glass temperature of porous hollow epoxy	99
Table 4.6	Rheometer properties of ENR composites and NR composites	107

Table 4.7	Hardness of PHE-ENR and PHE-NR composites, Shore A	108
Table 4.8	Modulus M100 and M300 of PHE-ENR and NR-PHE composites	112
Table 4.9	Tensile properties of PHE-LLDPE composites	121
Table 4.10	Melting properties from DSC of PHE-LLDPE composites	124
Table 4.11	Batch temperature and Torque of PHE-PS composites	125
Table 4.12	Glass transition properties of PS and PS composites	129
Table 4.13	TGA properties of PS and PS composites	130
Table 4.14	Batch temperature and Torque of PMMA composites	132
Table 4.15	Glass transition temperature of PHE-PMMA composites	137
Table 4.16	Improvement of PHECa/PHE-filled composites	138
Table 4.17	Tensile toughness of PHE-PS and PHE-PMMA composites	138
Table 4.18	Insoluble weight percentage of Soxhlet extraction	145
Table 4.19	Glass transition temperature of pPS-PHE composites	151
Table 4.20	Glass transition temperature of pPMMA-PHE composites	154
Table 4.21	TGA properties of pPS-PHE composites	157
Table 4.22	TGA properties of pPMMA-PHE composites	158
Table 4.23	Glass transition temperature of silica interlocked PHE	165
Table 4.24	Thermal properties – TGA of silica interlocked PHE	169
Table 4.25	Derivative peak of silica interlocked PHE	170
Table 4.26	Derivative peaks of PHE-MTEOS hybrids	172
Table 4.27	Surface are properties of PHE at different size	177
Table 4.28	Weight percent remaining after Soxhlet extraction	180
Table 4.29	TGA properties of 38MEB and 75MEB composites	185
Table 4.30	Glass transition temperature of 38ME, 53ME, 75ME, M5E and PMMA	191



## LIST OF FIGURES

Figure 1.1	Problems of sphere shape filler dispersed in polymer matrix; (a) delamination and (b) failure of the filler. (c) New concept of interlocking mechanism, inner curve of the hole prevents delamination (arrow 1) and failure (arrow 2).	4
Figure 2.1	Schematic model of the morphological transformations in filled polymers, occurring as the silica content increases from less than 10 wt % (A), to ca. 10 wt % (B), to over 20 wt % (C), to over 50 wt % (D). The line-shaded areas are the silica particles, while the black areas correspond to tightly bound polymer and the gray areas to loosely bound polymer. (Tsagaropoulos & Eisenberg, 1995).	14
Figure 2.2	The concept of segmental interaction with carbon black surface (Wolff et al, 1996)	14
Figure 2.3	Probable mechanism of interaction between filler particles and ionic groups in the restricted mobility region (Datta et al, 1996)	14
Figure 2.4	Schematic representation of the three types of polymer-clay composites (Joly et al, 2002)	15
Figure 2.5	The schematic of polymer chains interlocked porous hollow particle	16
Figure 2.6	TEM photographs of P(S-MAA) (MAA content, 10 mol %) particles before (a) and after (b) and (c) treated at 150°C for 3h at initial pH value of 10.5 adjusted with NH <sub>4</sub> OH (b) and ethanolamine (c) (Okubo et al, 1997).	17
Figure 2.7	OM micrographs of the formation of phenolic resin particles (X100) and the scheme of formation of porous-hollow particles (Hong et al, 2007)	18
Figure 2.8	SEM micrographs of two type of multiporous hollow particles (Hong et al, 2006)	19
Figure 2.9	Scanning electron microscope photographs of multihollow poly(methyl methacrylate) (PMMA) microcapsules cross-linked with 50 wt% ethylene glycol dimethacrylate (EGDMA): a surface image and b inner phase image. The calculated loading yield of monosodium phosphate (MSP) in the microcapsules was 5% (Kim et al, 2003)	20

Figure 2.10	SEM micrographs of CaCO <sub>3</sub> precipitates at pH 9.8 (Hakido et al, 2005)	22
Figure 2.11	Structures of dimer acids and polyamide Versamids (Adams & Gannon, 1985)	25
Figure 2.12	Reaction of dimer and DETA to form imidazoline (Johnson et al., 1985)	25
Figure 2.13	Reaction of epoxy resin and polyamide resin (Floyd, 1966)	26
Figure 2.14	Formation of epoxy resin-hardener networks (Adams & Gannon, 1985)	27
Figure 2.15	Scheme of the possible production routes of thermoset rubber/layered silicate nanocomposites (Varghese and Kargar – Kocsis, 2003)	30
Figure 2.16	Polystyrene structures	32
Figure 2.17	Poly(methyl methacrylate) structures	33
Figure 2.18	Emulsion, flocculation and coalescence schematic (Robins and Hibberd, 1998)	48
Figure 3.1	Flow chart of producing porous hollow epoxy	55
Figure 3.2	Flow chart of utilization of PHE as filler in composite, in-situ polymerization, sol-gel and size effect	58
Figure 3.3	In-situ polymerization of styrene/MMA and PHE flowchart	67
Figure 3.4	Rheometer curve of rubber compound	73
Figure 3.5	Sohlex extraction diagram; <b>1:</b> Stirrer bar <b>2:</b> Still pot <b>3:</b> Distillation path <b>4:</b> Thimble <b>5:</b> Solid <b>6:</b> Siphon top <b>7:</b> Siphon exit <b>8:</b> Expansion adapter <b>9:</b> Condensor <b>10:</b> Cooling water in <b>11:</b> Cooling water out	76
Figure 4.1	SEM of epoxy particles at different homogenizing temperature.	78
Figure 4.2	Calcium carbonate coated epoxy and coating epoxy particles at large scale.	80
Figure 4.3	SEM micrograph of PHE at low and high homogenizing speed	82

Figure 4.4	Porous hollow epoxy of homogenization for 2min, 3 min and 5 min	83
Figure 4.5	Epoxy particles at difference curing temperature.	84
Figure 4.6	PHE at different $\text{CaCO}_3$ contents.	86
Figure 4.7	SEM micrographs of EP50R and EP80R	87
Figure 4.8	(a) Viscosity of epoxy-polyamide- $\text{CaCO}_3$ and temperature with heating time, (b) viscosity versus temperature	89
Figure 4.9	The schematic illustration of formation porous hollow epoxy.	92
Figure 4.10	Density of PHECa (before HCl treatment) and PHE (after HCl treatment)	95
Figure 4.11	Effect of $\text{CaCO}_3$ on particle size of PHE	96
Figure 4.12	BJH cumulative adsorption and desorption pore diameter (4V/A) of PHE	99
Figure 4.13	DSC curves of PHE of E50R, E100R and EP50R	100
Figure 4.14	TGA of PHE of E50R, E100R and EP50R	101
Figure 4.15	SEM micrograph of interlocking mechanism between PHE and NR latex	102
Figure 4.16	Tensile strength and elongation at break of latex and PHE-NR latex composites	102
Figure 4.17	Modulus of latex and PHE-NR latex composites	103
Figure 4.18	Tensile curves of PHE-NR latex composite and NR latex	104
Figure 4.19	SEM micrograph of tensile fracture surface of 0E-LW and 8E-LW	105
Figure 4.20(a)	Tensile strength of ENR composites	109
Figure 4.20(b)	Elongation at break of ENR composites	109
Figure 4.21(a)	Tensile strength of NR composites	111
Figure 4.21(b)	Elongation at break of NR composites	111
Figure 4.22	Tensile fracture surface of ENR composites	113
Figure 4.23	Tensile fracture surface of NR5E composites	113

Figure 4.24	Tear strength of ENR composites	114
Figure 4.25	Tear strength of NR composites	114
Figure 4.26	Tear fracture surface of PHE-ENR , PHE-NR composite	115
Figure 4.27	Cross sectional surface of one PHE interlocking epoxy-polyamine matrix	116
Figure 4.28	(a) Tensile strength and (b) Elongation at break of epoxy composites	117
Figure 4.28	(c) Young modulus of epoxy composites	118
Figure 4.29	SEM micrograph of tensile fracture surface of epoxy composites.	119
Figure 4.30	Interlocking of PHE and LLDPE	120
Figure 4.31	(a) Yield strength and (b) Elongation at yield of LLDPE composites	121
Figure 4.32	Tensile fracture surface of PHE-LLDPE composites	122
Figure 4.33	DSC curves of 1 <sup>st</sup> scan and 2 <sup>nd</sup> scan of PHE-LLDPE composites	123
Figure 4.34	Batch temperature and Torque of PS composites	125
Figure 4.35(a)	Tensile strength of PHE-PS composites	127
Figure 4.35(b)	Elongation at break of PHE-PS composites	127
Figure 4.35(c)	Modulus of PHE-PS composites	127
Figure 4.36	Tensile fracture surface SEM micrograph of PHE-PS composites	128
Figure 4.37	DSC curves of PHE-PS composites	129
Figure 4.38	TGA curves and Derivative of PS and PS composites.	130
Figure 4.39.	Batch temperature and Torque of PMMA composites	133
Figure 4.40	(a) Tensile strength and (b) Elongation at break of PMMA composites	134
Figure 4.40	(c) Modulus of PHE-PMMA composites	135
Figure 4.41	Tensile fracture surface of M10EC and M10E composites	136
Figure 4.42	DSC curves of PHE-PMMA composites	137

Figure 4.43	Image of pPS-PHE beads produced by in-situ suspension polymerization	140
Figure 4.44	Image of pPMMA-PHE beads produced by in-situ suspension polymerization	141
Figure 4.45	BPO chemical structure	142
Figure 4.46	FTIR of PHE and PHE after reacted with BPO	143
Figure 4.47	SEM images of (a) PSEAB and (b) MEB composites at cutting surface	144
Figure 4.48	SEM images of PSEAB and MEB after Soxhlet extraction.	146
Figure 4.49	Molecular weight of pPS-PHE composites	147
Figure 4.50	Molecular weight of pPMMA-PHE composites	147
Figure 4.51	FITR of soluble part of pPS-PHE after 4 <sup>th</sup> Soxhlet extraction and PS-A	149
Figure 4.52	FTIR of insoluble part of pPS-PHE after 30h Soxhlet extraction	150
Figure 4.53	FITR of soluble part of MEB after 1 <sup>st</sup> and 4 <sup>th</sup> extraction and insoluble part	151
Figure 4.54	DSC curves (second scan) of pPS-PHE composites.	152
Figure 4.55	DSC curves (second scan) of pPMMA-PHE composites.	154
Figure 4.56	DSC curves of pPMMA-PHE	155
Figure 4.57	pPMMA-PHE beads after DSC heating up to 350°C.	155
Figure 4.58	TGA properties of pPS-PHE composites, (a) TGA, (b) Derivative	156
Figure 4.59	TGA curves and Derivative curves of pPMMA-PHE composites	158
Figure 4.60	XRD of pPS-PHE and pPMMA-PHE composites	160
Figure 4.61	Silica and polyalkoxysilanes from TMOS, TEOS, MTEOS and PTEOS.	161
Figure 4.62	Silica prepared from TMOS with different PHE contents	162
Figure 4.63	Silica prepared from TEOS with different PHE contents	

Figure 4.64	Polysiloxane of MTEOS and PTEOS with 10% PHE	163
Figure 4.65	DSC curves of silica-PHE hybrids	164
Figure 4.66	DSC curves of PHE- MTEOS hybrid	165
Figure 4.67	(a) TGA curves and (b) Derivative curves of silica-PHE	166
Figure 4.68	(a) TGA curves and (b) TGA derivative curves of PHE-MTEOS hybrids	167
Figure 4.69	SEM micrograph of 40ESiE	171
Figure 4.70	ESi0 before and after TGA up to 900°C	172
Figure 4.71	SEM micrograph of 40MSiE and 40ESiE after TGA up to 900°C	173
Figure 4.72	The morphology of silica interlocked PHE (or the dovetail pin of silica)	173
Figure 4.73	SEM micrograph of PHE at different sizes	174
Figure 4.74	BJH cumulative adsorption and desorption pore diameter (4V/A) of PHE at different size	176
Figure 4.75	Cutting surface of 38MEB and 75MEB beads	178
Figure 4.76	SEM micrograph of 38MEB and 75MEB after 4 <sup>th</sup> cycle extraction	179
Figure 4.77	Molecular weight of 38MEB and 75MEB	180
Figure 4.78	FTIR of insoluble 38MEB and 75MEB	181
Figure 4.79	DSC curves of 38MEB and 75MEB	182
Figure 4.80	DSC curves of 38MEB and 75MEB up to 350°C	183
Figure 4.81	TGA curves and Derivative of 38MEB and 75MEB	184
Figure 4.82	Torque and batch temperature of 38ME, 53ME and 75ME	185
Figure 4.83	Tensile properties of 38ME, 53ME and 75ME (a) tensile strength and elongation at break, (b) modulus	186
Figure 4.84	SEM micrograph of tensile fracture surface of 38ME, 53ME and 75E at 100X	187
		189

Figure 4.85	SEM micrograph of tensile fracture surface of 38ME, 53ME and 75E at 1000X	190
Figure 4.86	DSC curves of 38ME, 53ME, 75ME, M5E and PMMA	191
Figure 4.87	Surface of PE10E after tensile test (white arrow shows tensile load direction)	192
Figure 4.88	The schematic illustration of interlocking mechanism under tensile load, (1) in direction, (2) & (2') perpendicular and oblique	193
Figure 8.89	The illustration of interlocking direction with PHE and PMMA matrix of tensile fracture surface: (1) in direction, (2) & (2') perpendicular and oblique	194
Figure 4.90.	Deformation mode of interlocking, (a) pulling out of and maintaining NR interlocking PHE (b) pulling out of and deformed LLDPE interlocking PHE	195
Figure 4.91	Breaking the neck of the interlocking PS matrix	195
Figure 4.92	Breaking PHE particles interlocking PMMA matrix	196

## LIST OF ABBREVIATION

12F-PE	Fluorinated poly(aryl ether ketone)
AFM	Atomic force microscope
AIBN	2,2 –azobisisobutyronitrile
Al <sub>2</sub> O <sub>3</sub>	Aluminum oxide
AN	Monomeric Acrylonitrile
ASP	Alkali Swelling Procedure
ATBN	Amine-terminated butadiene-acrylonitrile
BA	Butyl acrylate
BET	Brunauer, Emmett & Teller (1938)
BHT	2,6-di-tert-butyl-p-cresol
BPO	Benzoyl peroxide
CaCl <sub>2</sub>	Calcium chloride
CaCO <sub>3</sub>	Calcium carbonate
CIPS	Chemically Induced Phase Separation
CNT	Carbon nanotube
CO <sub>2</sub>	Carbon dioxide
CTBN	Carboxyl-terminated butadiene-acrylonitrile
DEGDA	Diethylene glycol diacrylate
DETA	Diethylenetriamine
DGEBA	Diglycidyl ether of bisphenol A
DLA	Diffusion-limited aggregate
DNA	Deoxyribonucleic acid
DPP	Diphenylolpropan



DRC	Dry rubber content
DSC	Differential Scanning Calorimetry
DSM	Dynamic Swelling Method
ECH	Epichlorohydrin
ee <sub>w</sub>	epoxide equivalent weight
EGDMA	ethylene glycol dimethacrylate
ENR	Epoxidised natural rubber
EPDM	Ethylene Propylene Diene rubber
ETBN	Epoxy-terminated butadiene-acrylonitrile rubber
FTIR	Fourier transform infrared spectroscopy
GPC	Gel Permeation Chromatography
HBP <sub>s</sub>	Dendritic hyperbranched polymers
HCl	Hydrochloride acid
IPN	A semi-interpenetrating polymer network
KOH	Potassium hydroxide
LCD	Liquid crystal display
LLDPE	Linear low density polyethylene
LS	Pristine layer silicate
MAA	Methacrylic acids
MBT	2-mercapto-benzothiazole
MgSO <sub>4</sub>	Magnesium sulfate
MMA	Methyl methacrylate
MMT	Montmorillonite
MTEOS	CH <sub>3</sub> Si(OC <sub>2</sub> H <sub>5</sub> ) <sub>3</sub> - Methyl triethyl orthosilicate
Na <sub>2</sub> HPO <sub>4</sub>	Sodium hydrogen phosphate

Na <sub>2</sub> SO <sub>4</sub>	Sodium sulfate
NaCl	Sodium chloride
NaHSO <sub>3</sub>	Sodium sulfite
NaOH	Sodium hydroxide
NH <sub>3</sub>	Ammonia
NH <sub>4</sub> OH	Ammonium hydroxide
NR Latex	Natural rubber latex
NR	Natural rubber
O/W	oil-in-water
O/W/O	oil-in-water-in-oil
OLS	Organophilic layer silicate
OP10	Rapeseed oil
P(S-MAA)	Styrene-methacrylic acid copolymer
PBA	Polybutylacrylate
PBT	Poly(butadiene terephthalate)
PC	Poly(carbonate)
PCL	Poly(ε-caprolactone)
PEEK	Poly(ether ether ketone)
PEI	Poly(ether imides)
PEO	Poly(ether oxide)
PEPO	Polyether-phosphineoxide
PES	Poly(ether sulfones)
PET	Polyethylene terephthalate
PI	Polyimide
PMMA	Poly(methyl methacrylate)

PPE	Poly (2,6-dimethyl-1,4-phenylene ether)
PPE	Poly(2,6-dimethyl-1,4-phenylene ether)
PPO	Poly(phenyl oxide)
PS	Polystyrene
PTEOS	$C_5H_6Si(OC_2H_5)_3$ - Phenyl triethyl orthosilicate
PU	Poly(urethane)
PVA	Poly (vinyl alcohol)
SaPSeP	Safe-assembling of Phase Separated Polymer
SBR	Styrene-Butadiene-Rubber
SC CO <sub>2</sub>	supercritical carbon dioxide
SDBS	Sodium Dodecyl Benzene Sulfonate
SEM	Scanning Electron Microscope
SiO <sub>2</sub>	Silicon dioxide
SMR	Standard Malaysian Rubber
SPG	Shirasu Porous Glass
TEM	Transmission electron microscopy
TEOS	$Si(OC_2H_5)_4$ - Tetraethyl orthosilicate
TGA	Thermogravimetric analysis
TMOS	$Si(OCH_3)_4$ - Tetramethyl orthosilicate
TMTD	Tetramethyl thiuram disulphide
TOFAS	Tall oil fatty acids
TPs	Thermoplastics
W/O	water-in-oil
W/O/W	water in oil in water
wpe	weight per epoxide
XRD	X-ray diffraction
ZnO	Zin oxide

# **PENGHASILAN DAN PENGGUNAAN EPOKSI BERLIANG GERONGGANG DENGAN KAEDAH BERASASKAN AIR SEBAGAI PERNGISI TERMAJU**

## **ABSTRAK**

Epoksi berliang geronggang (PHE) telah dihasilkan melalui kaedah berasaskan air dan digunakan sebagai pengisi di dalam polimer bagi meningkatkan “sifat-sifat bersama” pengisi dalam komposit. PHE telah dihasilkan dengan membenarkan ketidaklengkapan cantuman titisan kecil epoksi dalam emulsi, yang mana disediakan melalui penghomogenan campuran epoksi, poliamida dan kalsium karbonat dalam air. Partikel epoksi ini selepas dimatangkan adalah poros, berongga dan berbentuk seperti sfera. Lubang pada partikel epoksi boleh diisi dengan matrik polimer untuk membentuk pengikatan antara partikel epoksi dan polimer. Pengikatan ini menjamin interaksi yang lebih baik dan pengigi ini berpotensi untuk digunakan sebagai pengisi penguat. Mekanisma pengikatan ini adalah suatu konsep yang baru dan “novel”.

Untuk penyediaan komposit, tiga jenis polimer yang akan digunakan sebagai matrik telah dipilih: Elastomer: lateks NR, NR, dan ENR; termoset: poliamina termatang epoksi ; termoplastik; LLDPE, PS dan PMMA. Keputusan menunjukkan pengikatan telah diperolehi untuk semua matrik polimer yang digunakan. Polimer yang berbeza akan menghasilkan mod kegagalan yang berbeza terhadap pengikatan. Secara am, terdapat tiga mod kegagalan dicadangkan, yang mana telah diklasifikasikan sebagai tertarik keluar (kekalkan morfologi *interlocked* dan ubahbentuk morfology *interlocked*) pemutusan matrik pada leher pengikatan dan pemutusan PHE. Pengikatan juga mempengaruhi sifat termal komposit. Komposit boleh menahan haba dengan baik memandangkan epoksi adalah bahan rintangan haba yang baik kerana ia mempunyai rangkaian sambung silang tiga dimensi. PHE

boleh mempengaruhi pergerakan rantai polimer dan ini memberi kesan terhadap pengurangan suhu peralihan kaca termoplastik (LLDPE, PS dan PMMA).

Pempolimeran in-situ dijalankan untuk menyelidik kesan PHE terhadap suspensi stirena/metil metakrilat (MMA) juga untuk proses sol-gel. Pengikatan melalui lubang epoksi antara PHE dan PS/PMMA adalah berjaya diperolehi melalui mikrograf SEM. PHE telah didapati bertindak balas dengan BPO dan membantu pempolimeran stirena dan MMA. Tambahan lagi, kesan PHE telah dilihat ke atas pempolimeran MMA dengan memberi kesan terhadap berat molekul berbeza yang diperolehi pada dalam dan luar lubang epoksi. Walaubagaimanapun, kesan adalah tidak begitu jelas untuk pempolimeran stirena disebabkan ketidakpolarannya. Untuk proses sol-gel, keputusan TGA mempamerkan kandungan silika yang sama ditinggalkan oleh PHE dan sampel PHE *interlocked*, jadi boleh dikatakan PHE mempunyai kesan sangat rendah kepada proses sol-gel.

Kesan saiz partikel dan morfologi lubang PHE terhadap pempolimeran suspensi MMA dan pencampuran leburan dengan PMMA telah diselidik. Penggunaan PHE yang sedikit memberikan kesan dalam peningkatan berat molekul PMMA diperolehi. Walaubagaimanapun, sifat termal tidak menunjukkan perbezaan yang ketara. Untuk komposit percampuran leburan PMMA, keputusan adalah menarik iaitu partikel PHE yang besar menunjukkan sifat tensil yang sedikit meningkat. Terdapat tiga jenis PHE dalam saiz 38-53  $\mu\text{m}$ , 53-75  $\mu\text{m}$  dengan kurang lubang, dan 75-106  $\mu\text{m}$  dengan lubang berganda. Partikel penguat optimum adalah pada saiz 53-75  $\mu\text{m}$ . Boleh dibuat kesimpulan bahawa PHE dengan bilangan lubang yang optimum dan saiz lubang yang optimum boleh menjadi pengisi penguat yang bagus, dimana ia dapat memperbaiki semua sifat tensil seperti kekuatan tensil, pemanjangan pada takat putus begitu juga modulus.

# **PRODUCTION AND UTILIZATION OF POROUS HOLLOW EPOXY BY WATER-BASED METHOD AS AN ADVANCED FILLER**

## **ABSTRACT**

Porous hollow epoxy - PHE was produced by water based method and used as filler in polymer in order to improve the “collaborative properties” of filler in composites. The PHE was produced by allowing the incomplete coalescence of epoxy tiny droplets in emulsion, which was prepared by homogenizing the mixture of epoxy, polyamide and calcium carbonate in water medium. These epoxy particles after cured are porous, hollow and spherical. The holes on epoxy particle could be filled by the polymer matrix to form interlocking between epoxy particle and polymer. The interlocking should be promising better interaction and has potential to be used as reinforcing fillers. This interlocking mechanism is a new and novel concept.

To prepare composites, the polymer used as matrix were chosen in three types: elastomers: NR latex, NR and ENR; thermoset: epoxy cured polyamine; thermoplastic: LLDPE, PS and PMMA. The results showed the interlocking was obtained for all of the used polymer matrix. The mechanical properties were maintained or enhanced depending on the used polymer. Different polymer would result in different failure modes of the interlocking. In general, there are three proposed failure modes, which were classified as pulling out (maintain interlocked morphology and deform interlocked morphology), matrix broken at interlocking neck, and PHE broken. The interlocking was also effect thermal properties of composites. Composite could endure better heat since epoxy is a good heat resistance material due to its three dimension crosslink networks. PHE could affect to polymer

chain mobility resulting in slight reduction of glass transition temperature of thermoplastic (LLDPE, PS and PMMA).

In-situ polymerization was carried out to investigate the effect of PHE on suspension of styrene/methyl methacrylate (MMA) as well as sol-gel process. The interlocking through epoxy holes between PHE and PS/PMMA was successfully obtained as SEM photo of cutting surface pPS-PHE and pPMMA-PHE beads. PHE had found to react with BPO and retard the polymerization of styrene and MMA. Moreover, the effect of PHE had found on polymerization of MMA reflecting on different molecular weight obtained at inner and outer epoxy hole's. However, the effect could not be apparent for styrene polymerization due to its non polarity. For sol-gel process, TGA results exhibited a similar portion of silica remained of non PHE and interlocked PHE samples, so it could be said that PHE could have very low effect to sol-gel process.

The effect of particle size and hole's morphology of PHE on suspension polymerization of MMA and melt blending with PMMA was investigated. The use of smaller PHE resulted in higher molecular weight of PMMA obtained. However, thermal properties did not show an obvious difference. For PMMA melt blending composites, it is interesting that larger PHE particle expressed slightly higher tensile properties. There are three types of PHE in the size of 38 – 53  $\mu\text{m}$ , and 53 – 75  $\mu\text{m}$  with less holes, and 75 – 106  $\mu\text{m}$  with multiple holes. It could be said that they are small particle with less medium holes, medium particle with medium holes, and large particle with many small holes. The optimum reinforcement particle is 53 – 75  $\mu\text{m}$ . It concluded that a PHE with optimum number of holes and optimum hole's size would be a good reinforced filler, which improved better all tensile properties such of tensile strength, elongation as well as modulus.

## CHAPTER 1

### INTRODUCTION

#### 1.1 Overview

The incorporation of filler into polymer to prepare a desired composite is the most attractive investigation for plastic applications. Composite properties would usually be tailored based on their filler properties. In general, two categories of filler properties are of interest in filled composites: “collaborative properties” and “self properties”. “Collaborative properties” influence dispersion and interaction of filler to matrix including surface features and morphology of filler, whilst “self properties” are additional properties obtained by the resultant composites such as mechanical, thermal, conductive, chemical properties, etc. Both reflect the original characteristic of filler: morphology, physical and chemical structures.

Commonly, filler is usually exploited for their “self properties” in composite. “Collaborative properties”, which decide the type of plastic which the filler could be incorporated, are often neglected and the focus is usually on filler treatment as well as on coupling agents.

Demonstrating for the exploitation of self properties is rubber toughening of epoxy and other brittle plastics. The study focused on the elasticity of rubber in order to enhance fracture resistance. Typical elastomers those are used for this system are liquid rubber butadiene-acrylonitrile (CTBN, ATBN and ETBN) (Chikhi et al., 2002; Robinette et al., 2004; Thomas et al., 2007). The toughening effect is achieved but there are some drawback of decreasing stiffness, strength and thermal properties of epoxy composites. In order to improve these drawbacks the introduction of high  $T_g$



thermoplastic as a toughening agent such as polysulphone, phenylmaleimide, polystyrene, hydroxyl terminated poly (ether ether ketone) etc. are explored (Mimura et al., 2001; Giannotti et al., 2003; Francis et al., 2005; Hernandez et al., 2007; Gong et al., 2008). However, the toughening efficiency was lower compared to the liquid rubber modified epoxy.

The addition of preformed core-shell particles in the plastic by in-situ polymerization of monomer is exploited to partially surmount this difficulty (Duguet et al., 2000; Nguyen-Thuc and Abderrahim, 2002; Becu et al., 2002; Luna-Xavier et al., 2004; Tang et al., 2006; Dzunuzovic et al., 2007). The morphology and properties of core-shell particles can be tuned in advance, so that the composite could be prepared in predetermined morphology and independent of the curing process. Nevertheless, there is a drawback of limited size of core-shell particles (in the range of 100-500nm) (Woo & Hseih, 1998; Minami et al., 2005).

## **1.2 Multiporous hollow particles**

In order to increase the contact area between matrix and filler, commonly the filler will be reduced in size such as from micron filler to nano-scale filler. The use of nano filler is normally challenging in term of obtaining good dispersion and to overcome favourable agglomeration. The other effects of nano filler are safety and health factors since nano filler is possible to be inhaled and can even cause endosmosis through human skin. Other material of higher surface area is hollow microsphere, which has been widely applied in packing system as packing material for chromatography column and spacer spheres for liquid crystal display (LCD), polymer-supported catalyst, polymer-immobilized extractant, templates of preparing porous inorganic microsphere, carrier of

enzymes and drugs (Omi et al. 1997). However, its utilization as reinforcing filler is less investigated.

The common method to produce hollow microspheres are alkali swelling procedure (ASP), dynamic swelling method (DSM), Shirasu porous glass (SPG) membrane technique, and water-in-oil-in-water (W/O/W) emulsion polymerization technique which involve the use of organic solvents or oil and using microfluidics (Shah et al., 2008). Blending of hollow microspheres with other polymer could be limited or less adherence. The use of supercritical carbon dioxide (SC CO<sub>2</sub>) as a foaming agent to generate porous polymer materials was reported to avoid the solvent-removing processes, but the method needs high pressure vessel and high pressure pump. Based on the method of safe-assembling of phase separated polymer (SaPSeP) at the interphase of the droplets of SaPSeP, Minami et al. (2005) succeeded to synthesis cured epoxy resin particles having one hole at interface with water.

### **1.3 Problem statement**

#### **1.3.1 Common porous hollow particles**

The microspheres have closed cell structure and possess fewer holes at the surface which make them not suitable for interlocking with matrix. The hollow structure sizes in these methods are quite small, the cell walls are also thin and these factors may interfere interlocking mechanism and subsequently results in a weak interlock. Moreover, the production process involves to oil and solvent, hence the interaction of the porous hollow particles and matrix could be weak. Inorganic microsphere usage is also reported and it works quite similar to common filler and the term of interlocking is not really obvious (Calisle et al., 2007).

### 1.3.2 Chemically induced phase separation

In all above systems, the toughening efficiency is strongly depended on chemically induced phase separation but it is difficult to control and obtain a stable the morphology of final toughened particles. It could be said the “collaborative properties” of these systems is weak and needed improvement. In these composites, polymer particles are firstly dispersed as filler in a continuous polymer matrix where polymer particles play a role to suppress the crack tip in the matrix via the aid of difference in hardness and toughness between filler and polymer matrix (Zhang et al., 2009). For example, general toughening plastic by using sphere shape particles are as follows, (i) delamination at interface between filler and matrix (Figure 1.1 (a)), and (ii) failure of the filler due to a break into the filler (Figure 1.1 (b)).

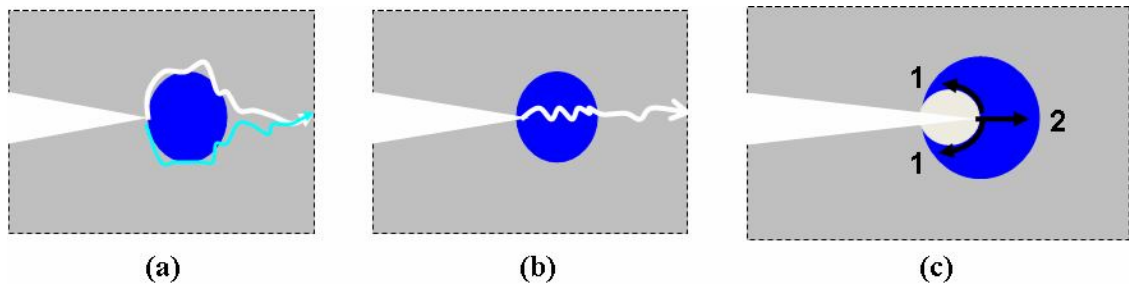


Figure 1.1 Problems of sphere shape filler dispersed in polymer matrix; (a) delamination and (b) failure of the filler. (c) New concept of interlocking mechanism, inner curve of the hole prevents delamination (arrow 1) and failure (arrow 2).

### 1.4 Porous hollow epoxy

In this study, a novel water based method is introduced to prepare micro epoxy particles having not only one but many holes (micro sizes) at the surface. The toughness and stiffness of epoxy particles can be obtained by varying the ratio of epoxy and polyamide. This method is relatively simple and environmental friendly because no

solvent is used and the possibility of production on a large scale is high. The presence of more than one hole in micro size is very promising since it has potential to be used as reinforcing fillers, which can be filled with matrix through interlocking mechanism. This advanced filler leads to a prospect of multiple function filler applied not only for epoxy matrix but also for other types of matrix such as elastomers and even for non-polymer matrix like ceramic and alumina. Besides interlocking application, the porous hollow epoxy can also be used as a drug or DNA carrier in bio-science.

The holes can be filled with matrix to form interlocking and consequently the composite properties were enhanced via this interlocking mechanism which is considered as a new and novel concept. The special characteristic of this filler incorporation in a polymer is that epoxy phase of the filler is cured and independent from curing process of the matrix. These particles are porous and hollow so that the morphology of dispersed epoxy into polymer will result in better dispersion and interaction composite material. The porous hollow epoxy exhibits better collaborative properties via its morphology and surface features. The interlocking mechanism that could happen is as suggested in Figure 1.1 (c) previously.

For porous hollow epoxy filled matrix, the interlocking mechanism expresses its reinforcement based on the type of polymer matrix. Possible failure of interlocking mechanism could be suggested as:

- i. Pulling out but able to maintain interlocked morphology for such flexible and toughened elastomers. Pulling out but unable to maintain interlocked morphology with elongated features such found in flexible and fiber forming thermoplastic.

- ii. No pulling out but neck breaking of the interlock such found in weak elastomers, brittle thermoplastic and thermoset.
- iii. Breakage of porous hollow structure due to high adhesion between epoxy and matrix.

### **1.5 Objectives of the study**

The objectives of the study are to produce the porous hollow epoxy particles by water-based method and propose the formation mechanism of porous hollow structure. The ability of porous hollow epoxy as filler is studied by preparing composites through common process such as casting, two-roll mill, internal mixer (Brabender, Haake), hot press, in-situ polymerization and sol-gel method. Through that, the interlocking practicability of porous hollow epoxy is proven with other type of polymers such as NR latex, elastomer (NR, ENR), thermoset (epoxy cured polyamine), thermoplastic (LLDPE, PS, PMMA) and inorganic (Silica). Furthermore, the effect of interlocking on mechanical properties and thermal properties of are investigated. The failure mode under tensile and tear of interlocking of porous hollow epoxy in different polymers are observed. Lastly, the effect of different particle size and porous hollow structure on in-situ polymerization and melt blending composite are studied.

## **CHAPTER II**

### **BACKGROUND AND LITERATURE REVIEW**

#### **2.1 Fillers**

##### **2.1.1 Functions of filler in composites**

The definition of filler in Handbook of filler (Wypych, 2000) is “Filler is a solid material capable of changing the physical and chemical properties of materials by surface interaction or its lack thereof and by its own physical characteristics”. From this definition, it could be suggested that filler works more than as an additive. The use of filler in a polymer matrix is very common in polymer composite in order to reduce the cost, reinforcement, alter the processing method. The choice of filler depends on the application of polymer. In fact, nowadays, the use of filler is not simply as the way to reduce cost but to obtain the specific properties of the composites. Properties of filler will be exploited via the combination of filler and plastic.

##### **2.1.2 Type of fillers**

There is some classification of fillers. The most common classification of fillers is according to their mineral origin and their chemical composition (mineral, glass, carbon black, organic, metal). Nowadays, more fillers are studied, synthesized and introduced to research and industry so the division of fillers which is based on filler characteristic could be more suitable. Fillers can also be divided based on their particles sizes (micro-sizes, nano-sizes), or their morphology (common shape, irregular, particles, fiber.). Fillers can be grouped in application through their properties such as mechanical, thermal, electrical, magnetic, fluorescence, opacity as

well as degradability, bio-degradable. This classification is more propagated nowadays in researches and industries.

### **2.1.3 Filler properties**

The overall value of a filler is a complex function of intrinsic material characteristics, such as average particle size, particle shape, intrinsic strength, and chemical composition; of process-dependent factors, such as particle-size distribution surface chemistry, particle agglomeration, and bulk density; and of cost. Abrasion and hardness properties are also important for their impact on the wear and maintenance of processing and molding equipment (Mark, 2004). Here are some typical properties of a filler, which have influences on filler dispersion, loading and mechanical properties of composites (Wypych, 2000; Mark, 2004).

#### **i. Chemical composition**

Fillers can be inorganic or organic and of an established chemical composition. Filler can also be a single element, natural products, synthetic filler, mixtures of different materials in unknown proportions (waste and recycled materials), or materials of a proprietary composition.

#### **ii. Physical state**

Most of fillers are used in solid state or can be as a dispersed state. Filler can be in liquid state of monomer or solvent dissolved state which is used in the process of in-situ polymerization, sol-gel methods, rubber toughening plastic and polymer toughening plastic.

#### **iii. Morphology of filler**

Filler can have these morphologies such as spherical, cubical, irregular, block, plate, flake, fiber, mixtures of different shapes and also hollow or porous. The

shape of an individual particle has great impact on the flexural modulus, permeability, and flow behavior of a filled polymer. Spherical particles give the highest packing density, a uniform distribution of stress, increase melt and powder flow, and lower viscosity. Cubic and tabular shapes give good reinforcement and packing density. Dendritic particles have a very large surface area available for interaction. Flakes have large reflecting surfaces, facilitate orientation, and lower the permeability of liquids, gases and vapors. Elongated particles give superior reinforcement, reduce shrinkage and thermal expansion and facilitate thixotropic properties. Irregular particles may not possess special advantages but they are generally easier to make and are thus considered as inexpensive fillers.

#### **iv. Particle size and aspect ratio**

Filler size can range from a few nanometers to millimeters. Nano-filler is more focused recently because better electron microscopy equipment (SEM, TEM, AFM) are available. It could be said that sub-nano filler can be investigated in future whenever it can be evident and proven using laboratory equipments. Nanoparticles, with dimensions ranging up to 100 nm, deliver the strongest enhancements only when they are properly dispersed. Due to increases in both the surface area and the corresponding surface area to volume ratio with a reduction in filler particle size, finer particles are prone to agglomerate for the conservation of internal energy and are more difficult to be dispersed. The particle size is actually based on one dimension of the filler and the estimation is related to the determination methods themselves. Particle size determination is complicated by size distribution, the presence of particle associations, and the shape of particles. For those particles in irregular shape, it is difficult to express their dimensions. The method used for particle size determination (sieving, light scattering, microscopy) determines what



dimensional aspects are measured. For hollow filler particles, the dimension of holes and porous is essential for the interlocking application.

The aspect ratio, or the ratio of the longest length of particle to its thickness, is most commonly used to measure the shape of a filler particle. The aspect ratio of a sphere was the lowest and equal to 1.0. The aspect ratio increases with a filler's shape progresses from a sphere to a block, to a plate, or to a flake. The filler loading content and dispersion depends on this aspect ratio.

#### **v. Particle size distribution**

Particle size distribution of filler can be monodisperse, designed mixture of sizes, Gaussian distribution or irregular distribution. In polymer composites, the particle size distribution of the filler has influence on viscosity and on loading content of filler during incorporation. In some plastics, a certain stress distribution is required and, in such cases, monodisperse, spherical particles are best. Changes to the particle size distribution will change the undertone of the pigment allowing a system to be tailored to the requirements. Certain grades may be capable of providing optical brightening or of masking the yellow color.

#### **vi. Surface area**

Surface area is a very important parameter of filler. Surface area value varies depending on the measurement methods. BET is the reasonable methodology for surface area measurement. The surface area depends on particle size, morphology and porosity. The specific surface area determines the contact surface between filler and matrix and influences significantly mechanical properties of the composites (Pukanzsky, 1996).

### **vii. Wetting and coupling properties**

Wetting and dispersion of filler are critically depended on the chemical compatibility between filler surface and matrix, which affects directly to physical performance of filled polymer. According to water affinity, filler surfaces are usually classified as hydrophilic or hydrophobic. Mineral fillers can be coated or chemically treated with hydrophobic wetting agents to modify their surface chemistry to aid their dispersion in nonpolar polymer. The modification with wetting agents also restricts agglomeration of filler so allow for higher filler loadings with lower viscosities during filler incorporation. The wettability can also be estimated by the contact angle measured between a drop of water or oil and the filler surface.

### **viii. Hardness**

The effect of filler to polymer hardness depends on the interaction between filler and polymer. Soft filler (such as rubbers toughen rigid plastic) is able to enhance fracture toughness.

### **ix. Mechanical properties**

Strong mechanical filler could prevent a failure of tear or break filler so the mechanical properties of composites will depend on interaction of filler and matrix.

### **x. Other properties**

pH of filler also affects the dispersion in polymer. The high particle – particle interaction and attraction will lead agglomeration and causes a poor dispersion of filler in matrix. The thermal conductivity of filler and its concentration are the main parameters determining the thermal conductivity of composite. Thermal expansion coefficient affects the dimensional stability of composites. Thermal expansion can be used as simple method of verifying the adhesion between the filler and the matrix. If the adhesion is poor the composite will have high thermal expansion. Beside that, the

blending processing is influenced by the thermal conductivity of filler, especial organic filler and its melting temperature (Wypych, 2000).

In general, these properties of filler are essential to take into account for synthesis of a new filler for polymer. Depending on the desired properties of composites, the selected properties of filler can be tailored. The focus is necessary not only on the enhanced properties (self properties) but also the interaction of filler to matrix (collaborative properties). In this study, interaction of filler is improved by the increase in surface area and the introduction of the new interlocking mechanism, which is achieved by exploiting the porous hollow structure of the produced filler.

#### **2.1.4 Interactions**

The properties of composites are critically dependent on the interface between the filler and the matrix polymer. The type of interface depends on the character of the interaction which can be either physical or chemical in nature. Both types of interactions contribute differently to the reinforcement of polymeric materials. Formation of chemical bonds in filled materials generates enhanced physical properties. An interfacial bond improves interlaminar adhesion, delamination resistance, fatigue resistance, and corrosion resistance. These properties are dependent on shape, size and functional group distribution of filler. The filler surface acts as a template for interface formation which allows the reactivity of the filler surface to come into play. Morphology of filler decides the surface area of filler, which can be in the form of spherical, cubical, block, flake, fiber (Wypych, 2000). There are two important factors in filler composites which are dispersion of filler in matrix and the interaction between them. Interaction is a complex process involving:

- A chemical reaction between the filler and matrix materials
- Physical interaction (van der Waals forces and hydrogen bonding)
- Changes in morphology of interacting components
- Mechanical interlocking

These processes modify surface layers of both interacting materials (filler and matrix) and form an interphase which differs in properties from the bulk matrix. The formation of the interphase is responsible for changes in the physical and mechanical properties of filled materials and usually improves material reinforcement.

It is suggested that three models of interaction between the surface of the filler and the matrix, which are mainly based on the types of fillers used. The first model is according to the typical report of Tsagaropoulos & Eisenberg (1995), which is shown in Figure 2.1. The filler particles of lower or about 10 wt% is surrounded by a tightly bound polymer covered by a layer of loosely bound chains. As the loading increases, the areas of loosely bound polymer begin to overlap, consisting the entire matrix to be influenced by the filler. If filler loading is high, there is little space left for loosely bound polymer and the participation of the layers of tightly bound polymer increases. At different filler loadings, a change in the interaction mechanism is likely to occur.

The second model of interaction between the surface of the filler and the matrix is the rubber chain attaches to carbon black (Figure 2.2). The rubber chain can be attached at single points (a), multiple points (b) and connected two or more carbon black particles. Reactive functional groups can be positioned in the middle of chain or at its ends and the reactions may involve chain segment or terminal group.

The third model is the report from Datta et al. (1996). The authors proposed a model of chemical interactions for a system of carbon black and maleated EPDM as

shown in Figure 2.3. The links could be hydrogen bonding and covalent bonding, which are characterized by the attachment of filler particles to the chain. Because the rubber is crosslinked, there is more opportunity for it to form interaction.

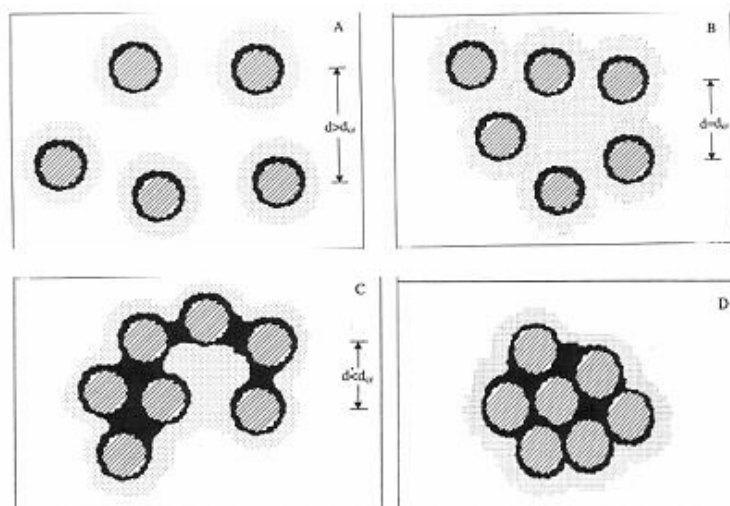


Figure 2.1. Schematic model of the morphological transformations in filled polymers, occurring as the silica content increases from less than 10 wt % (A), to ca. 10 wt % (B), to over 20 wt % (C), to over 50 wt % (D). The line-shaded areas are the silica particles, while the black areas correspond to tightly bound polymer and the gray areas to loosely bound polymer. (Tsagaropoulos & Eisenberg, 1995).

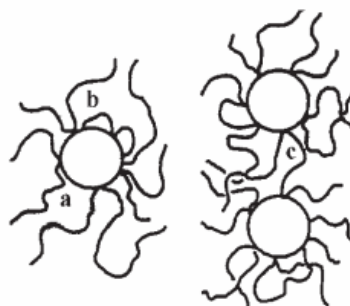


Figure 2.2. The concept of segmental interaction with carbon black surface (Wolff et al., 1996)

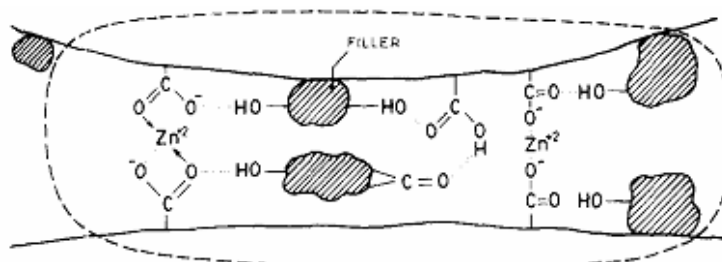


Figure 2.3 Probable mechanism of interaction between filler particles and ionic groups in the restricted mobility region (Datta et al., 1996)

The interaction of filler and matrix is usually improved by using coupling agents which are suitable for both filler and matrix. The use of smaller particles is also preferred to increase the contact area between matrix and filler, commonly the size of filler will be reduced such as from micron filler to nano-scale filler.

. The most common nano-filler is montmorillonite clay which has a crystal structure of layered silicate. For such filler, it required a modification on the clay so that the composites could obtain nano structure of filler and have a good dispersion of filler. If energetically favorable interactions exist between the modified silicate and the polymer, then the polymer chains can be inserted between the silicate layers, further increasing the interlayer spacing and leading to an ordered multilayer with a repeat distance of a few nanometers. If the polymer and the silicate are not compatible, agglomerates of layered silicate surrounded by polymer are formed. Thus, in the use of such clays as fillers in polymer systems, three general types of composite materials may be obtained (Figure 2.4): (a) conventional composites containing clay tactoids of stacked layers in a coplanar orientation associated in aggregates and agglomerates dispersed as a segregated phase, (b) intercalated nanocomposites, and (c) exfoliated nanocomposites (Joly et al., 2002).

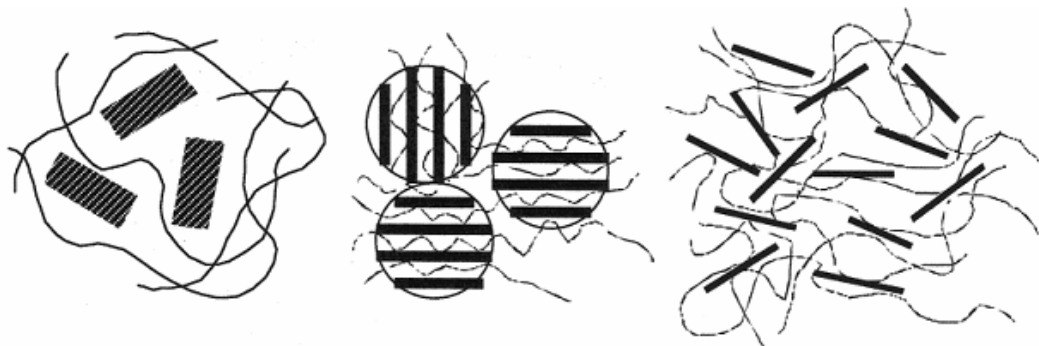


Figure 2.4. Schematic representation of the three types of polymer-clay composites (Joly et al., 2002)

For mechanical interlocking, Gorl et al. (1996), who investigated the size of voids in fumed silica in its original form and after compounding with rubber, suggest that the increase in the size of pores depended on the conditions of mixing and on the formulation of rubber. Reinforcement required the initial size of silica pores to be large enough to allow penetration by rubber chains.

Interlocking of polymer matrix and filler is rather new, we propose the schematic of how the polymer chains attach to filler in Figure 2.5. In general, interlocking is a macroscopic phenomenon, which actually consists of common interaction of polymer chains to filler surface. Here, the enhancement comes from higher surface area of filler as well as the dovetailing effect which is similar to snap button mechanism.



Figure 2.5 The schematic of polymer chains interlocked in porous hollow particle

#### **2.1.5 Porous hollow particles**

As high surface area materials, hollow microspheres have been widely applied as packing materials for column chromatography and spacer spheres for liquid crystal display (LCD), polymer-supported catalysts, polymer-immobilized extractants, templates of preparing porous inorganic microspheres, and carriers of enzymes and drugs (Omi et al. 1997). However, the use of hollow micropores as reinforcing filler is not widely investigated.

There are numerous reports to produce porous hollow particles by various methods. The common methods to produce hollow microspheres are alkali swelling

procedure (ASP) , dynamic swelling method (DSM) (Okubo et al., 1996), Shirasu porous glass (SPG) membrane technique (Omi et al., 2000) and water-in-oil-in-water (W/O/W) emulsion polymerization technique which involve the use of organic solvents or oil (Kim et al., 1999, Kim et al., 2003). Lee et al. (2008) reported a multihollow structure of poly(methyl methacrylate)/silver nanocomposite microspheres prepared by suspension polymerization in the presence of dual dispersion agents. The hollow particles obtained with different hole sizes which are dependent on the concentration of surfactant Arlacel P135.

Alkali/cooling method to produce multihollow polymer particles was proposed by Okubo et al. (1996 & 1997). Styrene with 10wt% of methacrylic acids – MAA was allowed to emulsion polymerize at 70°C. The emulsion of over 95% conversion was diluted and adjusted to pH 12.0 with alkali aqueous solution and then was heated by dipping in oil bath at 150°C for 3h. After the treatment, each emulsion was cooled under the room temperature. The alkali treatment could react with trapped MAA to produce holes on the particles. The holes were observed under TEM as closed holes and in nano size (Figure 2.6)

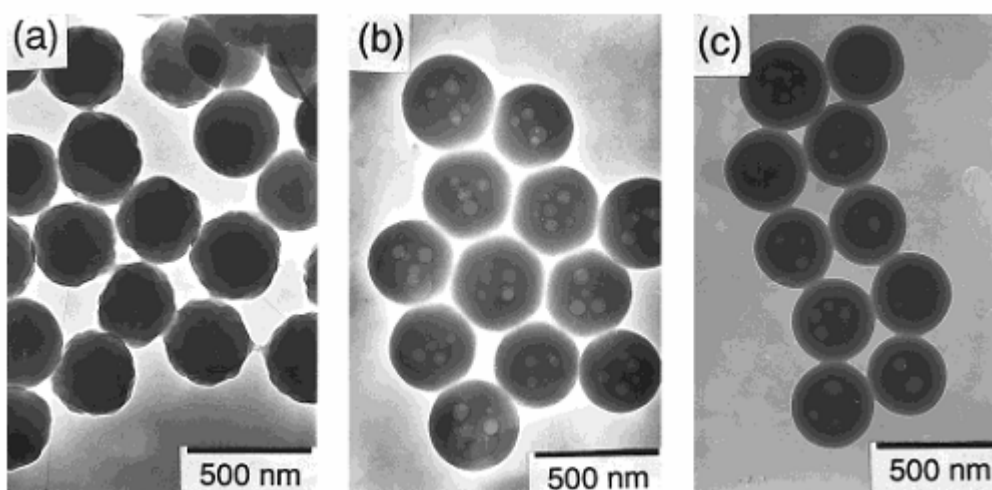


Figure 2.6 TEM photographs of P(S-MAA) (MAA content, 10 mol %) particles before (a) and after (b) and (c) treated at 150°C for 3h at initial pH value of 10.5 adjusted with NH<sub>4</sub>OH (b) and ethanolamine (c) (Okubo et al., 1997).



Hong et al. (2007) reported a preparation of porous/hollow phenolic particles by suspension polymerization from a resol, water-soluble phenolic resin in a multiple emulsion system oil-in-water-in-oil (O/W/O) (Figure 2.7). The water-soluble phenolic resin was synthesized via condensation of phenol and formaldehyde with an alkaline catalyst to have a 50wt% resol precursor solution. Rapeseed oil, OP10 and resol solution were mixed in the homogeneous solution to get the O/W pre-emulsion, which was dropped slowly into the reaction kettle containing rapeseed oil and Span 80 (to obtain O/W/O system). The polymerization was carried out continuously at 130°C for 4h in N<sub>2</sub> atmosphere. The porous particles obtained were spherical particles contained voids or bubbles. These are closed voids and porous particles looked similar to closed cell.

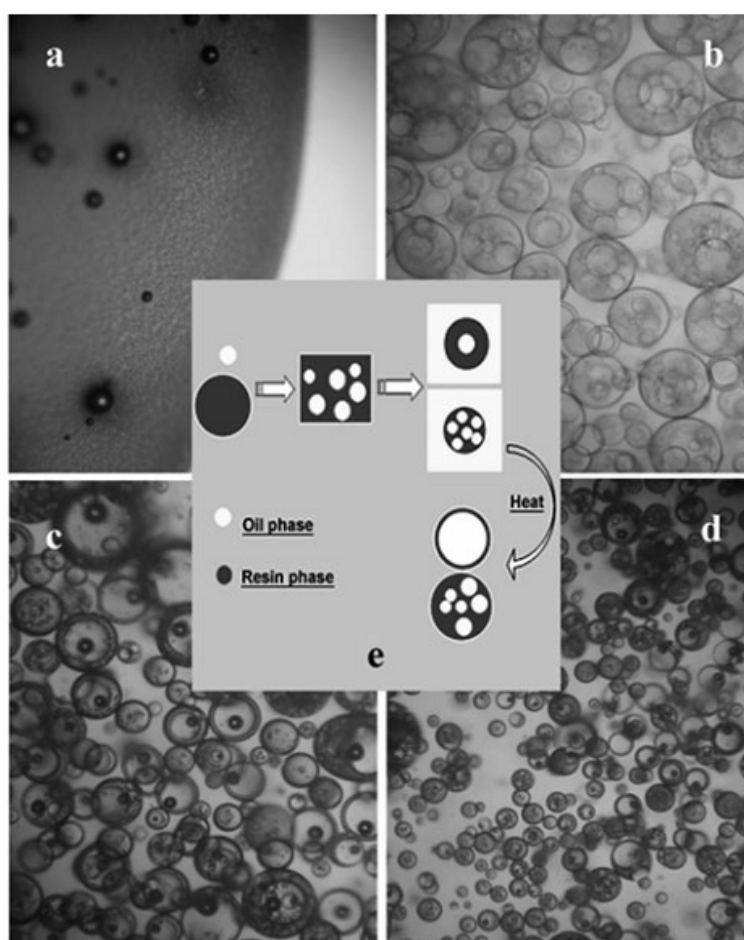


Figure 2.7 OM micrographs of the formation of phenolic resin particles (X100) and the scheme of formation of porous-hollow particles (Hong et al., 2007)

Hong et al. (2006) fabricated PMMA/butyl acrylate – BA porous microsphere through the emulsion polymerization in company with a phase inversion process. Mixture of monomer of MMA/BA, initiator and additives was charged a round-bottomed reactor equipped with a mechanical stirrer, a reflux condenser, thermocouples, and an N<sub>2</sub> inlet system. Solution of sodium hydrogen phosphate (Na<sub>2</sub>HPO<sub>4</sub>) sodium dodecyl benzene sulfonate (SDBS), poly (vinyl alcohol) and water was dropped slowly into the reactor at a given agitation speed to drive phase inversion. Then the polymerization was carried out continuously at 65°C for 4h. The porous particle obtained was similar to an open foam particle in spherical, which have numerous of connected holes and thin side walls (Figure 2.8).

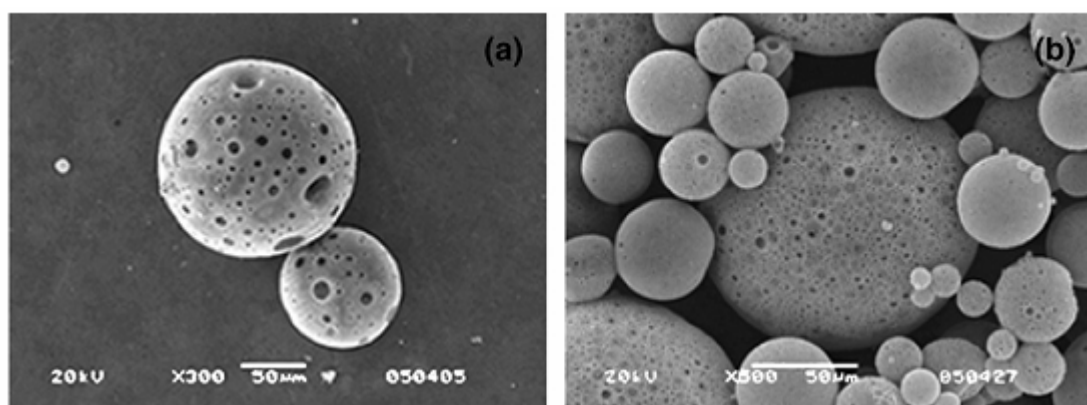


Figure 2.8 SEM micrographs of two type of multiporous hollow particles (Hong et al., 2006)

Kim et al. (2003) described the methodology of production of multihollow polymer microcapsules by water-in-oil-in-water emulsion polymerization. W/O/W emulsion polymerization was carried out by modifying the two-step emulsion procedure. First, a W/O emulsion was prepared as follows aqueous solution containing a model water-soluble ingredient was dropped into an oil phase composed of MMA, EGDMA monomer and additives. Then, the water/oil mixture was homogenized. The W/O emulsion prepared was a milky viscous phase. Second, the

W/O emulsion was re-dispersed by homogenizing it mildly in 1wt% PVA aqueous solution, obtaining finally a stable W/O/W emulsion. Right after the preparation of the W/O/W emulsion, the emulsion was transferred into a double-walled glass reactor to polymerize at 60°C for 10h under N<sub>2</sub> inlet system. The inhibition of polymerization in the aqueous phase is required. As shown in Figure 2.9, the particles were porous of multi close holes and no holes present on particles surface, so the application should not applicable for interlocking mechanism.

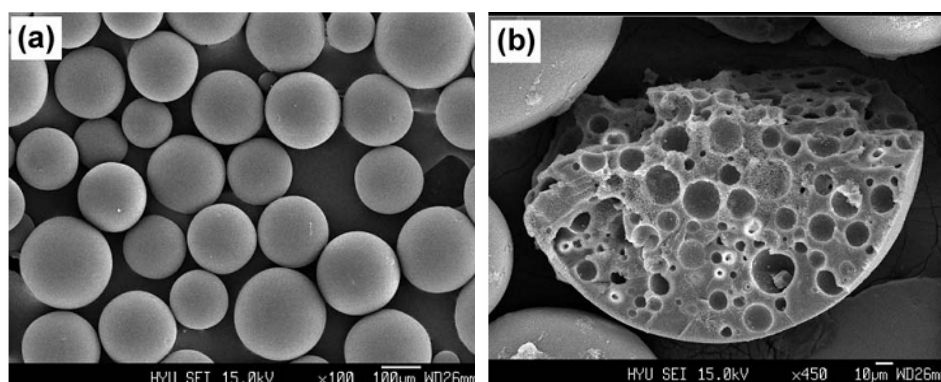


Figure 2.9 Scanning electron microscope photographs of multihollow poly(methyl methacrylate) (PMMA) microcapsules cross-linked with 50 wt% ethylene glycol dimethacrylate (EGDMA): a surface image and b inner phase image. The calculated loading yield of monosodium phosphate (MSP) in the microcapsules was 5% (Kim et al., 2003)

Most studies of W/O/W emulsions have dealt with the stabilization of active ingredients and their sustained-release properties. A serious problem can be found in that there have been few works that satisfy the requirements for wide application. The reasons for this are their intrinsic thermodynamic instability and low active ingredient entrapment efficacy. To overcome all those failures of W/O/W emulsions, a stable W/O/W is essential.

The use of supercritical carbon dioxide (SC CO<sub>2</sub>) (Sun et al., 2004, Huang et al., 2007) as a foaming agent to generate porous polymer materials was reported to avoid the solvent-removing processes, but the method needs to utilize high pressure vessel and high pressure pump.

Recently, Shah and his colleagues (2008) reviewed and introduced the designer emulsions using microfluidics. The glass capillary devices were used to generate single, double, and higher order emulsions which can serve as ideal templates for producing well-defined particles and functional vesicles. The method is needed to engineer pathways to scale up the production.

All the above methods exploit the entrapment of the other unmingled components in monomer phase. The polymerization and further removing process are used to form hollow structure. All these methods also bring some drawbacks: complex treatment procedures and industrial waste, which lead to much time wasting and consumption. The membrane technique to produce microspheres through polymerization of the monomer emulsion using Shirasu porous glass (SPG) is complex method.

Liu et al. (2007) produced micro hollow microspheres by suspension polymerization of Styrene-DEGDA (diethylene glycol diacrylate) with petroleum ether (90 – 120°C), but there is single hole on the particles. The possibility of production in large scale is not promising. The microspheres are closed cell and have less micron size holes at the surface which make them not suitable for interlocking with matrix. The hole sizes in these methods are quite small, and the cell walls are also thin which subsequently restricts the formation of interlock and results in weak interlocking. Moreover, blending of these hollow microspheres with other polymer could be limited or low adherence due to the oil phase.

Inorganic microspheres are also reported by several workers, and they were quite similar to common filler and the term of interlocking is not really obvious (Kim et al., 2001, Liang et al., 2007, Calisle et al., 2007, Liu et al., 2009). Hakido et al. (2005) reported the synthesis of hollow calcium carbonate by bubble templating

method. Hollow  $\text{CaCO}_3$  particles were produced by using bubble as template via passing  $\text{CO}_2$  bubbles into calcium chloride ( $\text{CaCl}_2$ ) solution in the presence of ammonia ( $\text{NH}_3$ ) at  $27^\circ\text{C}$ . The  $\text{CO}_2$  bubble is not only the reactive material, but also the template for the hollow particles. The newly-formed primary particles were attached to the bubbles and formed a solid shell. After filtering and drying, hollow  $\text{CaCO}_3$  particles were obtained. This hollow  $\text{CaCO}_3$  is similar to a  $\text{CaCO}_3$  balloon and the broken particle would show an empty core as seen in Figure 2.10b.

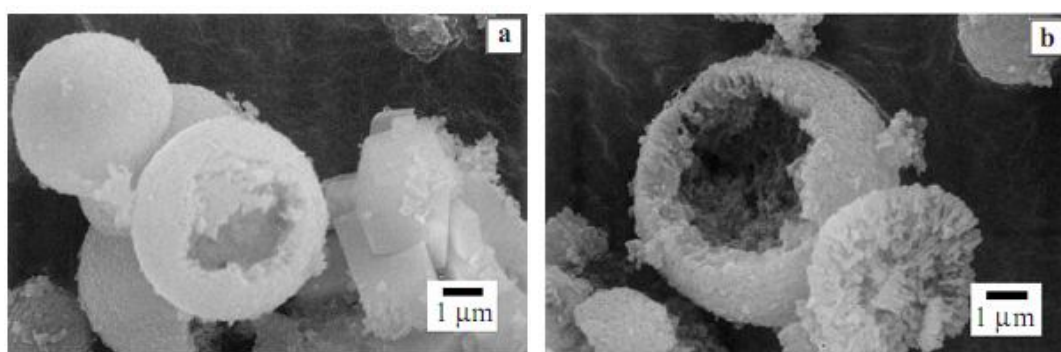


Figure 2.10 SEM micrographs of  $\text{CaCO}_3$  precipitates at pH 9.8 (Hakido et al., 2005)

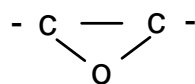
Based on the method of safe-assembling of phase separated polymer at the interphase of the droplets SaPSeP, Minami et al. (2005) succeeded to synthesise cured epoxy resin particles having one hollow at interface with water. The presence of polystyrene (PS) dissolving in epoxy/diamine/toluene droplets are exploited to promote the phase separation of the epoxy reacted with the diamine. PS needs to be prepared by solution polymerization with 2,2'-azobisisobutyronitrile as initiator. When the PS did not dissolve in the droplets, no hollow particles were obtained. There were certain minimum values of the PS content and its molecular weight to obtain the hollow particles. In this case, polyvinyl (vinyl alcohol) (PVA) is also needed as a colloidal stabilizer.

In the present work, a novel water based method is introduced to prepare micro epoxy particles having not only one but many holes (micron sizes) at the surface. The toughness and stiffness of epoxy particles can be obtained by varying the ratio of epoxy and polyamide (Du, 2003). This method is so simple and environmental friendly because no solvent is used and the possibility of production on a large scale is high. The presence of more than one hole in micron size is very promising since it has potential to be used as reinforcing fillers, which can be filled with matrix through interlocking mechanism. This advanced filler leads to a prospect of multi function filler applied not only for epoxy matrix but also for other types of matrices such as elastomers, thermoplastic and even for non-polymer matrices like ceramic and alumina. Besides interlocking application, porous hollow epoxy can also use as a drug or DNA carrier in bio-science but with a caution of bio-degradable.

## **2.2 Epoxy and Polyamide**

### **2.2.1 Epoxy**

Epoxyes are thermoset resins and are characterized by a three-membered oxide ring known as epoxy, epoxide, oxirane or ethoxyline group:



The epoxy ring is susceptible to attack from a wide variety of substances to form the crosslinked three dimensional networks in the end product. There are many types of epoxy resins such as: epichlorohydrin-bisphenol A, phenoxy resins, epoxy novolac resin, halogenated epoxy resin, hydrogenated bisphenol A resin, Among them, liquid epichlorohydrin-bis phenol A resin is the most important resin and have wide applications due to the low viscosity and easy processing. As can be seen from

its name, epichlorohydrin-bisphenol A is the product of the condensation of epichlorohydrin (ECH) with diphenylolpropan (DPP) which is also called bisphenol A in the presence of NaOH as catalyst. Epichlorohydrin behaves as a difunctional monomer, the epoxide group can be opened by hydroxyl group of bisphenol and the halohydrin can be dehydrohalogenated by alkali. The ratio of epichlorohydrin and bisphenol A has an effect on the average molecular weight of the liquid resin (Adams & Gannon, 1985). Uncured liquid epoxy is mainly characterized by the epoxy content, viscosity, color, density, hydrolysable chlorine and volatile content. The epoxy content is expressed as weight per epoxide (wpe) or epoxide equivalent weight (eew), which is defined as the weight in gram which contains one gram equivalent of epoxide.

### **2.2.2 Curing with polyamide**

Vegetable oil-polyamide resins are also called Versamids. Versamids were introduced in the early 1950's, have dark colour, ranging from viscous liquids to brittle resins and with varying solubility. These polyamides have found usage as hardeners-cum-flexibilisers for epoxy resin (Brydson, 1975). Polyamide Versamids are condensation products of fatty dibasic acid (C-13, C-19, C-21 and C-36) and di-polyfunctional amines. Most of reactive polyamide is prepared from dimer acids, and diethylenetriamine (DETA).

Dimer acids (polymerized vegetable oil acids) are usually prepared from tall oil fatty acids (TOFAS). The reaction that formed dimer acids occurs under heating, steam pressure and chemical catalyst. The structure of dimer acid is shown in Figure 2.11 (Adams & Gannon, 1985).